IEEE Access
Multidisciplinary | Rapid Review | Open Access Journal

Received July 13, 2020, accepted August 2, 2020, date of publication August 14, 2020, date of current version August 27, 2020.

Digital Object Identifier 10.1109/ACCESS.2020.3016697

Low Complexity Iterative Receiver With Lossless Information Transfer for Non-Binary LDPC Coded PDMA System

HANQING DING[1], QINGQING LIU[2], ZIHANG DING[3], JIN XU[1], ZHE ZHANG[1], WEIHUA LIU[1], (Member, IEEE), AND XUEYAN CHEN[1]

[1]School of Computer and Communication Engineering, Zhengzhou University of Light Industry, Zhengzhou 450001, China
[2]School of Information and Electronics, Beijing Institute of Technology, Beijing 100081, China
[3]International Education College, Zhengzhou University of Light Industry, Zhengzhou 450001, China

Corresponding author: Hanqing Ding (dinghanqing@zzuli.edu.cn)

This work was supported in part by the Henan Province important project in Colleges and Universities under Grant 18B510019 and Grant JSJ20190097; in part by the National Natural Science Foundation of China under Grant 61901418; and in part by the Science and Technology Research Project of Henan Province under Grant 202102210124 and Grant 202102210122.

ABSTRACT In this work, we first proposed a non-binary low-density parity-check (NB-LDPC) coded pattern division multiple access (PDMA) scheme with the order of the Galois field equal to the size of modulation alphabet which can avoid the symbol-to-bit or bit-to-symbol probability conversion between the detector and decoder as in binary coded system. Specifically, we considered a 4-ary LDPC over Galois field (GF(4)-LDPC) coded PDMA system with quadrature phase shift keying (QPSK) modulation. At the receiver side, Gaussian approximation based message passing (GAMP) detection algorithm instead of standard message passing (SMP) is employed to achieve a tradeoff between the computational complexity and the detection performance. When iterative detection and decoding (IDD) algorithm is used, the symbol-wise extrinsic information of the detector and GF(4)-LDPC decoder can be exchanged without information loss. At last, we proposed a symbol-wise EXIT (S-EXIT) based iterative optimization algorithm to improve the system performance. Both the S-EXIT chart based analysis and numerical simulation results show the validity of the proposed scheme above.

INDEX TERMS PDMA, GAMP, NB-LDPC, IDD, iterative optimization.

I. INTRODUCTION

In current, non-orthogonal multiple access (NOMA) becomes a hot research topic in fifth-generation or beyond wireless communication system. The philosophy of NOMA is not only coincide with the information theory perspective to achieve multiple access channel capacity but also can support more users over limited resource which is important for high spectral efficiency and high throughput communication systems. In recent years, there are a large number of achievements have been reported on this issue. For example, in [1], a sparse spreading signature based NOMA scheme called low-density signature multiple access (LDSMA) is proposed, where a factor graph based message passing algorithm is used as multiple user detection (MUD) algorithm at the receiver side. The proposed sparse signature sequence combined with the message passing detection algorithm can efficiently reduce the computational complexity of the detector [2]. In [3], a modified NOMA scheme called pattern division multiple access (PDMA) is proposed, which employs unequal diversity pattern sequence to accelerate the convergence of the message passing based detector. The above two schemes employ the same kind of message passing based detection algorithm, which is referred to as standard message passing (SMP) algorithm in this paper. Take a closer look at the SMP algorithm, we find that the message updating at the function node decoder (FND) has an exponential computation complexity. When the system overload factor or the constellation size is large, the computational complexity is extremely high and sometimes becomes intolerable. In [4] and [5], Gaussian approximation based message passing algorithm (GAMP) has been used in multiple-input multiple-output (MIMO) system, especially in massive MIMO system, and shows effectiveness and

The associate editor coordinating the review of this manuscript and approving it for publication was Rui Wang.

advantage over traditional linear detection algorithm such as zero-forcing and minimum mean square error or theirs variants, in which case SMP algorithm is impractical. The difference between GAMP algorithm and SMP algorithm is that at the FND, the former models the received combined signal as Gaussian distributed random variable which thus leading to a linear computation complexity, while the later exhibits an exponential computation complexity since it is a chip-wise *maximum a posteriori* (MAP) detector.

Low-density parity check (LDPC) code constructed over Galois field (GF) of order q, i.e. GF(q)-LDPC, can achieve better performance than their binary counterpart especially in high order modulation system [6], [7]. However, a key issue obstacle non-binary LDPC from widely use is its underlying high decoding complexity if the GF order is high [8]. However, this drawback does not play a leading role in PDMA system with quadrature phase shift keying (QPSK) since we only consider LDPC code over low-order GF, i.e. GF(4)-LDPC code, which is of reasonable computational complexity. The main contributions are summarized in the following.

- We proposed a GF(4)-LDPC coded PDMA scheme with QPSK modulation constellation. Furthermore, GAMP based detection algorithm is employed to tradeoff the computation complexity and performance. GAMP algorithm has linearly complexity which is suitable for high overload case;
- GF(4)-LDPC decoder is of reasonable computation complexity and low memory consumption when compared with high order LDPC code such as $q \geq 16$, and can be coupled with the GAMP-based MUD seamlessly without information loss for QPSK system.
- We proposed a symbol-wise EXIT (SEXIT) chart based iterative optimization algorithm to further improve the receiver performance by optimizing the non-binary LDPC degree distribution.

In this paper, we use the same notation as in reference [5], in which $N_c(x; m, \sigma^2) \triangleq \frac{1}{\pi\sigma^2}\exp\left(-|\alpha - m|^2/\sigma^2\right)$ denotes a complex Gaussian probability density function, i.e. x is a complex Gaussian random variable with mean m and variance σ^2.

The remainder of this paper is organized as follows. In Section II, the system model of PDMA system is presented. Section III is about the SMP algorithm and low-complexity GAMP algorithm. In Section IV, the proposed symbol-wise iterative optimization algorithm is described in detail. Numerical results are presented in Section V, followed by concluding remarks in Section VI.

II. SYSTEM MODEL

In this work, we assume that orthogonal frequency division multiple (OFDM) is available for the uplink system. Consider a GF(4)-LDPC coded PDMA system with QPSK modulation, in which N_t users transmit over N_r resource elements (RE) to communicate to the base station (BS) simultaneously. For PDMA system, the system overload factor is defined as $\beta = N_t/N_r$ and $\beta > 1$ [9]. For each user, source bits are encoded with a GF(4)-LDPC encoder, then the coded symbols are directly mapped to QPSK constellation $\mathcal{A}$ according to LTE standard [10]. In the next step, spreading each QPSK symbol onto N_r REs using an user-specific pattern sequence (PS) with length N_r [11]. Let vector $\mathbf{s}_i = [s_{0,i}, s_{1,i}, \cdots, s_{N_r,i}]^T \in \{0,1\}^{N_r\times 1}$ denote the PS associated with user-i, where $s_{j,i} \in \{0,1\}$ denotes the j-th element of $\mathbf{s}_i$. Furthermore $\mathbf{S}_{N_r,N_t} = [\mathbf{s}_1, \mathbf{s}_2, \cdots, \mathbf{s}_{N_t}] \in \{0,1\}^{N_r\times N_t}$ denotes the pattern matrix (PM) of the PDMA system. As shown in Fig. 1, $\mathbf{S}_{2,3}$ and $\mathbf{S}_{3,6}$ are PMs corresponding to PDMA systems with 150% and 200% overload respectively [2]. At last, the derived signal is transmitted over wireless channel. For simplicity, we assume that all users and the BS are equipped with a single antenna. Furthermore, we consider the case that all users transmit with equal power, which is the worst situation in multiuser detection perspective. At the receiver side, the received signal associated with the N_r REs can be expressed as

$$\mathbf{y} = \sum_{i=1}^{N_t} \mathrm{diag}\,(\mathbf{h}_i)\,\mathbf{s}_i x_i + \mathbf{n}, \tag{1}$$

where $\mathbf{h}_i = [h_{1,i}, h_{2,i}, \cdots, h_{N_r,i}]^T \in \mathbb{C}^{N_r\times 1}$ is the $N_r \times 1$ complex-valued vector denotes the channel coefficients vector from user i to the BS over the N_r REs. More specifically, for $1 \leq j \leq N_r$, $h_{j,i}$ denotes the channel coefficient from user-i to the BS over RE-j. For vector $\mathbf{h}_i$, $\mathrm{diag}\,(\mathbf{h}_i)$ returns a diagonal matrix with diagonal given by $\mathbf{h}_i$. The $N_r \times 1$ vector $\mathbf{s}_i = [s_{0,i}, s_{1,i}, \cdots, s_{N_r,i}]^T$ is the PS of user i as aforementioned. Let x_i denote the transmitted modulation symbol of user-i, $\mathbf{n}$ is the N_r-dimensional Gaussian noise vector, i.e. $\mathbf{n} \sim CN\left(0,\ \sigma_n^2\mathbf{I}_{N_r}\right)$.

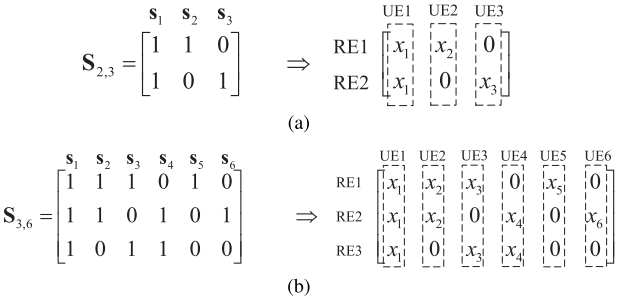

FIGURE 1. Pattern matrix of PDMA system (a) $\mathbf{S}_{2,3}$ for 150% overload (b) $\mathbf{S}_{3,6}$ for 200% overload.

For the j-th RE, the received baseband signal y_j can also be expressed as

$$y_j = \underbrace{h_{j,i}s_{j,i}x_i}_{\text{signal}} + \underbrace{\left(\sum_{\ell=1,\ell\neq i}^{N_t} h_{j,\ell}s_{j,\ell}x_\ell\right)}_{\text{interference}} + \underbrace{n_j}_{\text{noise}}, \tag{2}$$

where n_j is the j-th element of Gaussian noise vector $\mathbf{n}$ in (1), i.e. $n_j \sim CN\left(0,\ \sigma_n^2\right)$.

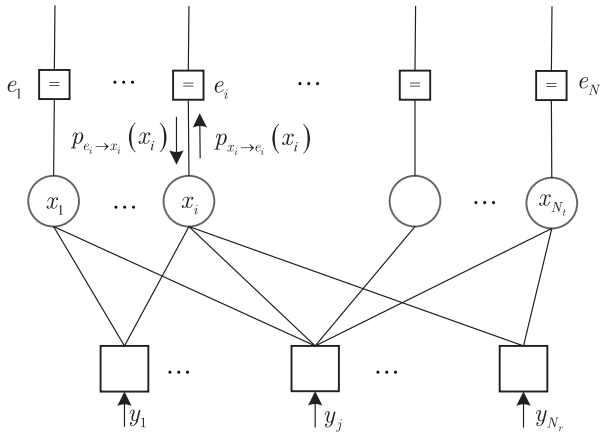

FIGURE 2. Factor graph of PDMA detector.

III. SYMBOL-WISE GAUSSIAN APPROXIMATION MESSAGE PASSING BASED MUD

In this section, we first give a review of the SMP algorithm and GAMP algorithm. It can be shown that for QPSK modulation and PDMA system, the computational complexity of the MUD can be significantly reduced by the Gaussian approximation.

A. QUASI-OPTIMAL STANDARD MESSAGE PASSING (SMP) BASED DETECTION ALGORITHM

Under factor graph framework, as shown in Fig. 2, the detector can be partitioned into two kinds of nodes, one is the function node decoder (FND) which associated with the received signal for each resource element (RE) y_j, $1 \le j \le N_r$, the other is the variable node decoder (VND) corresponding to the transmitted signal x_i, $1 \le i \le N_t$. The message passing algorithm operates with the extrinsic information exchanged between these two kinds of nodes iteratively along the edges. SMP algorithm can be described as formula (3) and (4) [12].

$$p_{x_i\to y_j}(x_i) = p_{e_i\to x_i}(x_i)\cdot \prod_{j'\in\chi(i)\backslash j} p_{y_{j'}\to x_i}(x_i), \tag{3}$$

$$p_{y_j\to x_i}(x_i) = \sum_{\mathbf{x}\in\chi(j)\backslash x_i}\left(f\left(y_j|\mathbf{x}\right)\prod_{i'\in\chi(j)\backslash i} p_{x_{i'}\to y_j}(x_{i'})\right), \tag{4}$$

where $p_{x_i\to y_j}(x_i)$ denotes the extrinsic probability information from variable node x_i to function node y_j, $p_{y_j\to x_i}(x_i)$ is the extrinsic probability information in opposite direction, and $f(y_j|\mathbf{x}) = \frac{1}{\pi\sigma_n^2}\exp(-|y_i - \sum_i h_{j,i}x_i|^2/\sigma_n^2)$. In the above two formulas, $\chi(i)\backslash j$ denotes the set of function node neighboring to variable node i except function node j. In principle, if the factor graph of the MUD is cycle-free, SMP can achieve the same performance as MAP algorithm. However, for large modulation alphabet size or high overload PDMA system, the SMP algorithm becomes impractical.

B. GAMP-BASED DETECTION FOR PDMA

1) MESSAGE PASSING FROM FND TO VND

As shown in formula (4), the calculation of the extrinsic information from FND y_j to VND x_i is of exponential computation complexity since we need to marginalize the joint distribution. The key point of GAMP algorithm is to model the input *a priori* message of FND $p_{x_{i'}\to y_j}$ (outgoing messing of VND) as continuous Gaussian random variable. Based on this idea, the extrinsic message passing from VND x_i to FND y_j is therefore approximated as Gaussian random variable, denoted as $p_{x_i\to y_j}(x_i) = N_c\left(x_i; m_{x_i\to y_j}, \sigma^2_{x_i\to y_j}\right)$, with mean $m_{x_i\to y_j}$ and variance $\sigma^2_{x_i\to y_j}$ [5]. As a result, the extrinsic information in probability manner can be expressed as

$$\begin{aligned} p_{y_j\to x_i}(x_i) &= \int_{\mathbf{x}\in\chi(j)\backslash i} f\left(y_j|\mathbf{x}\right)\prod_{x_{i'}\in\mathbf{x}} N_c\left(x_{i'}; m_{x_{i'}\to y_j}, \sigma^2_{x_{i'}\to y_j}\right) \\ &= N_c\left(x_i; m_{y_j\to x_i}, \sigma^2_{y_j\to x_i}\right), \end{aligned} \tag{5}$$

where $m_{y_j\to x_i}$ and $\sigma^2_{y_j\to x_i}$ denote the mean and variance of the Gaussian distributed extrinsic information $p_{y_j\to x_i}(x_i)$ from FND y_j to VND x_i respectively. According to (2) and (5), we have

$$m_{y_j\to x_i} = \left(y_j - \sum_{\ell\neq i} h_{j,\ell} m_{x_\ell\to y_j}\right)/h_{j,i}, \tag{6}$$

$$\sigma^2_{y_j\to x_i} = \left(\sum_{\ell\neq i}|h_{j,\ell}|^2\sigma^2_{x_\ell\to y_j} + \sigma_n^2\right)/|h_{j,i}|^2. \tag{7}$$

2) MESSAGE PASSING FROM VND TO FND

The incoming message of the VND x_i contains two types of probability information, one is the information, denoted as $p_{e_i\to x_i}(x_i)$, feedback from channel decoder, the other is the message transferred along d_v connected edges. To compute the extrinsic information delivered from variable node x_i to function node y_j, i.e. $p_{x_i\to y_j}(x_i)$, we need to perform the following three steps.

- **Step 1:** Calculate the distribution of the product of $d_v - 1$ input Gaussian distributed information except the j-th edge. Let $\tilde{m}_{x_i}$ and $\tilde{\sigma}^2_{x_i}$ denote the mean and variance of this combined Gaussian distribution $N_c\left(x_i; \tilde{m}_{x_i}, \tilde{\sigma}^2_{x_i}\right)$ respectively, according to the rule of the product of Gaussian distributions [13], $\tilde{m}_{x_i}$ and $\tilde{\sigma}^2_{x_i}$ can be computed as follows

$$\frac{1}{\tilde{\sigma}^2_{x_i}} = \sum_{j'\in\chi(i)\backslash j}\frac{1}{\sigma^2_{y_{j'}\to x_i}}, \tag{8}$$

$$\frac{\tilde{m}_{x_i}}{\tilde{\sigma}^2_{x_i}} = \sum_{j'\in\chi(i)\backslash j}\frac{m_{y_{j'}\to x_i}}{\sigma^2_{y_{j'}\to x_i}}. \tag{9}$$

- **Step 2:** Calculate the likelihood probability conditioned on the combined Gaussian distribution $N_c\left(x_i; \tilde{m}_{x_i}, \tilde{\sigma}^2_{x_i}\right)$ and the discrete *a priori* distribution $p_{e_i\to x_i}(x_i)$ feedback from channel decoder as following,

$$p_{x_i\to y_j}(x_i) = \frac{1}{\gamma}p_{e_i\to x_i}(x_i)\,N_c\left(x_i; \tilde{m}_{x_i}, \tilde{\sigma}^2_{x_i}\right), \tag{10}$$

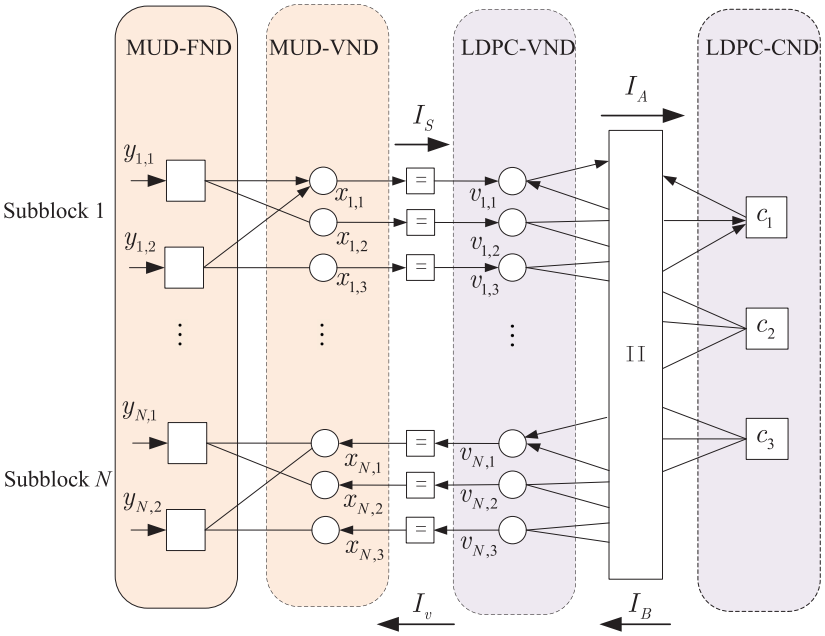

FIGURE 3. Joint factor graph of non-binary LDPC coded PDMA system.

where $\gamma = \sum_{x_i \in \mathcal{A}} p_{e_i \to x_i}(x_i) N_c\left(x_i; \tilde{m}_{x_i}, \tilde{\sigma}^2_{x_i}\right)$ such that $\sum_{x_i \in \mathcal{A}} p_{x_i \to y_j}(x_i) = 1$.

- **Step 3:** Approximate the discrete distribution $p_{x_i \to y_j}(x_i)$ in (10) with a continuous Gaussian distribution. To achieve this goal, we resort to moment matching as shown in [14] and [4]. The yielding continuous Gaussian distribution, denoted as $p_{x_i \to y_j}(x_i) = N_c\left(x_i; m_{x_i \to y_j}, \sigma^2_{x_i \to y_j}\right)$, with mean $m_{x_i \to y_j}$ and variance $\sigma^2_{x_i \to y_j}$ respectively can be evaluated as follows,

$$m_{x_i \to y_j}(x_i) = \sum_{\alpha \in \mathcal{A}} \alpha \cdot p_{x_i \to y_j}(x_i = \alpha), \tag{11}$$

$$\sigma^2_{x_i \to y_j}(x_i) = \sum_{\alpha \in \mathcal{A}} |\alpha|^2 p_{x_i \to y_j}(x_i = \alpha) - \left|m_{x_i \to y_j}(x_i)\right|^2, \tag{12}$$

where $\mathcal{A}$ denotes the constellation.

IV. PROPOSED JOINT FACTOR GRAPH BASED OPTIMIZATION

Since both GAMP detector and non-binary LDPC decoder can be depicted by factor graph, it is reasonable to represent the IDD receiver as a joint factor graph as shown in Fig. 3. A summary of the notations used is presented as follows,

- $y_{i,j}$: The j-th FND of the i-th subblock of MUD-FND.
- $x_{i,j}$: The j-th VND of the i-th subblock of MUD-FND.
- $v_{i,j}$: The VND of the LDPC code, i.e. LDPC-VND, and $v_{i,j} = x_{i,j}$ for analysis purpose.
- c_i: The CND of the LDPC code, i.e. LDPC-CND.
- I_v: The average mutual information (AMI) from LDPC-VND to MUD-VND.
- I_s: The AMI from MUD-VND to LDPC-VND.
- I_A: The AMI from LDPC-VND to LDPC-CND.
- I_B: The AMI from LDPC-CND to LDPC-VND.

The analysis and optimization of the non-binary LDPC coded PDMA system can be carried out under the joint factor graph framework by some powerful tools such as symbol-wise EXIT chart.

A. SYMBOL-WISE EXIT (S-EXIT) CHART BASED ANALYSIS

Extrinsic information transfer (EXIT) chart is widely used in the analysis and design of iterative detection and decoding (IDD) system. A lot of research work have demonstrated its effectiveness in predicting the threshold of IDD system [15], [16]. To obtain the EXIT chart of the iterative receiver, we first need to partition the receiver into some component detector/decoders. Then we evaluate the output AMI of the component detector/decoder with respect to the input *a priori* AMI. The derived functional relationship between the output and the input AMI is referred to as component-EXIT. When all component-EXIT charts are obtained, we can visualize the IDD system by a joint EXIT with all component-EXIT charts coupled according to their input and output relationship. Since it is difficult to track the actually exchanged message between the component decoders accurately. we resort to Monte-Carlo simulation aided symbol-wise EXIT analysis. The outline of this method can be summarized as follows. For each $I_A \in [0, 1]$, we model the *a priori* message according to formula (14). At the output of detector/decoder, we obtain the extrinsic information in terms LLR or probability manner, then we use formula (15) to calculate the output AMI I_E. The derived function I_E of I_A is the component-EXIT chart.

1) MODEL THE A PRIORI LLR AS $q-1$ DIMENSIONAL GAUSSIAN RANDOM VECTOR

If code symbol $v_i = 0$, i.e. $x_i = \mathcal{M}(0)$ is transmitted, where $\mathcal{M}(\cdot)$ is the mapping function from code symbol to constellation point, according to [16], the *a priori* LLR can be modeled as a q-1 dimensional Gaussian vector with mean $\mathbf{m} = \left[-\sigma^2/2 \cdots -\sigma^2/2\right]^T$ and covariance matrix $\mathbf{C}$ as

$$\mathbf{C} = \begin{bmatrix} \sigma^2 & & & \sigma^2/2 \\ & \sigma^2 & & \\ & & \ddots & \\ & & \sigma^2 & \\ \sigma^2/2 & & & \sigma^2 \end{bmatrix}. \tag{13}$$

Let Λ denote a q-1 dimensional Gaussian vector and $\Lambda \sim CN(0, \mathbf{I}_{q-1})$, then the *a priori* LLR $\mathbf{W}$ can be modeled as $\mathbf{W} = \mathbf{m} + \mathbf{C}^{\frac{1}{2}}\Lambda$ corresponding to $v_i = 0$. If $v_i = \alpha \in \{GF(q)\backslash 0\}$, then the corresponding *a priori* LLR of $x_i = \mathcal{M}(\alpha)$ can be modeled as

$$\begin{aligned} \mathbf{L} = \mathbf{W}^{-\alpha} &= \begin{bmatrix} w_{0-\alpha} - w_{-\alpha} \\ w_{1-\alpha} - w_{-\alpha} \\ \vdots \\ w_{q-1-\alpha} - w_{-\alpha} \end{bmatrix}_{q\times 1} \\ &\cong \begin{bmatrix} w_{1-\alpha} - w_{-\alpha} \\ w_{2-\alpha} - w_{-\alpha} \\ \vdots \\ w_{q-1-\alpha} - w_{-\alpha} \end{bmatrix}_{(q-1)\times 1}. \end{aligned} \tag{14}$$

The last equality is obtained by eliminating the first element of the q dimensional vector $\mathbf{L}$ since $w_{0-\alpha} - w_{-\alpha} = 0$.

2) THE CALCULATION OF THE OUTPUT AVERAGE MUTUAL INFORMATION

Instead of integrate the q-dimensional distribution, we resort to a numerical method which exploiting the ergodic characteristic of the transmitted code symbol. According to Theorem 2 in [17], we evaluate the output extrinsic AMI as follows

$$I_E \approx H(x) + \sum_{k=1}^{N}\sum_{\alpha=0}^{q-1} p\left(x_k|\mathbf{y}, \mathbf{L}_{\backslash k}\right)\cdot \log_q p\left(x_k|\mathbf{y}, \mathbf{L}_{\backslash k}\right). \tag{15}$$

where $H(x) = -\sum_{i=0}^{q-1} p(x=i)\log_q p(x=i)$ denotes the q-ary entropy function and $0 \le H(x) \le 1$, q is the order of the GF. With this definition, $H(x) = 1$ when x takes $\{0, 1, \cdots, q-1\}$ with equal probabilities. $p\left(x_k|\mathbf{y}, \mathbf{L}_{\backslash k}\right)$ is the output extrinsic information in probability manner at the output of the detector or decoder.

B. PROPOSED SYMBOL-WISE EXIT BASED ITERATIVE OPTIMIZATION ALGORITHM

Although GF(4)-LDPC code is employed, there is still ample room for improvement when iterative detection and decoding algorithm is used [18]. To facilitate the optimization,

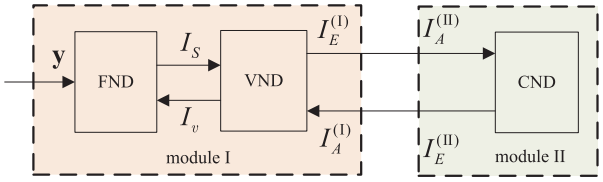

FIGURE 4. Block diagram of the IDD receiver.

we combine the FND module and VND module as module I, the CND individually is modeled as module II as shown in Fig. 4. In the following we will show how to obtain the component-EXIT corresponding to these two modules in detail. Let $\boldsymbol{\lambda} = \left[\lambda_2, \lambda_3, \cdots, \lambda_{D_v}\right]$ and $\boldsymbol{\rho} = \left[\rho_3, \rho_4, \cdots, \rho_{D_c}\right]$ denote the variable node degree distribution and check node degree distribution respectively, where D_v and D_c denote the maximum degree of VND and CND respectively, then the degree distribution pair $(\boldsymbol{\lambda}, \boldsymbol{\rho})$ gives a description of an ensemble of non-binary LDPC codes. The code rate of LDPC code is [19]

$$R = 1 - \frac{\sum_{i=2}^{Dv} \lambda_i/i}{\sum_{j=3}^{Dc} \rho_j/j}. \tag{16}$$

where $\lambda_i \ge 0$, $\rho_j \ge 0$, for $2 \le i \le D_v$ and $3 \le j \le D_c$, $\sum_{i=2}^{D_v} \lambda_i = 1$ and $\sum_{j=3}^{D_c} \rho_j = 1$.

1) CALCULATION OF THE EXIT CHART OF MODULE I

- The relationship between the input $I_A^{(\mathrm{I})}$ and output I_v of VDN can be expressed as

$$I_v = \sum_i \lambda_i J\left(\sqrt{d_{v,i}} J^{-1}\left(I_A^{(\mathrm{I})}\right)\right). \tag{17}$$

- The relationship between the output AMI I_s and input AMI I_v of FND can be denoted as

$$I_s = \phi\left(I_v,\ E_b/N_0\right). \tag{18}$$

  It can be seen from formula (18) that I_s is related to channel parameter E_b/N_0. This function can be obtained by Monte Carlo simulation. In Fig. 5, the relationship between I_v and I_s when E_b/N_0 changing from 3.5dB to 5.5dB with interval of 0.1dB for $\mathbf{S}_{2,3}$ PDMA system is shown.
- The relationship between the output AMI $I_E^{(\mathrm{I})}$ and the input AMI $I_A^{(\mathrm{I})}$ of module I, denoted as $I_E^{(\mathrm{I})} = f_1(I_A^{(1)})$, can be written as

$$\begin{aligned} I_E^{(\mathrm{I})} &= f_1(I_A^{(1)}) \\ &= \sum_i \lambda_i \sqrt{(d_{v,i}-1)^2 J^{-1}\left(I_A^{(\mathrm{I})}\right) + \left(J^{-1}(I_s)\right)^2}. \end{aligned} \tag{19}$$

2) CALCULATION OF THE EXIT CHART OF MODULE II

Let $I_E^{(\mathrm{II})}$ and $I_A^{(\mathrm{II})}$ denote the output and input AMI of module II respectively. For each $I_A^{(\mathrm{II})} \in [0, 1]$, we need to model the *a priori* LLRs of CND according to formula (14). For a

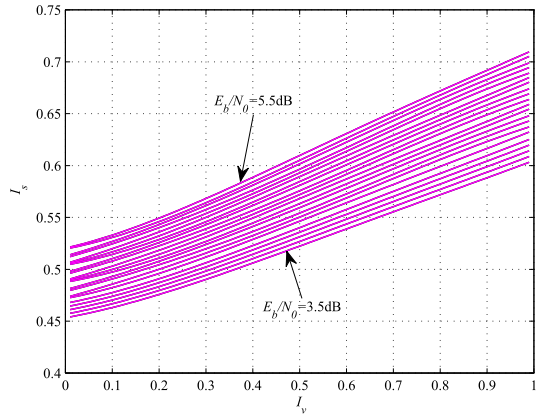

FIGURE 5. The functional relationship between I_S and I_V with differennt E_b/N_0 obtained by monte-carlo simulation.

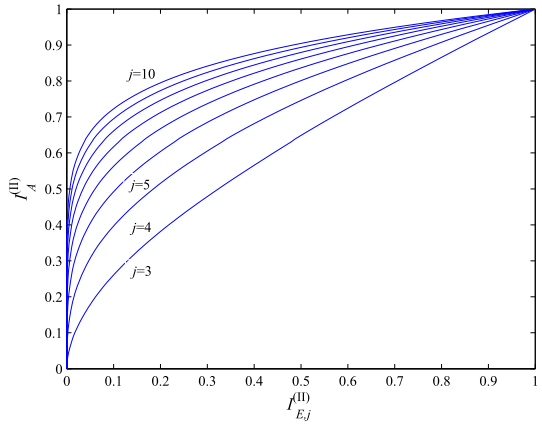

FIGURE 6. The EXIT curve of CND with different check node degree.

specifical check node degree j, the output extrinsic LLR can be obtained by numerical simulation, then the output AMI can be evaluated using formula (15). By curve fitting, we can obtain the function $I_{E,j}^{(\mathrm{II})} = h_j(I_A^{(\mathrm{II})})$ for each considered check node degree j. Fig. 6 gives an example of the CND curves with check node degree from j=3 to 10 for GF(4)-LDPC code. Thus, for all check node degree $j \in [3, D_c]$, the combined EXIT chart can be written as

$$I_E^{(\mathrm{II})} = f_2(I_A^{(\mathrm{II})}) = \sum_{j=3}^{D_c} I_{E,j}^{(\mathrm{II})} = \sum_{j=3}^{D_c} h_j(I_A^{(\mathrm{II})}). \quad (20)$$

Then the symbol-wise EXIT chart based iterative optimization algorithm can be summarized as Algorithm 1. The optimization process can be implemented with the simple linear programing algorithm [20]. It is need to point out that we can find the near-optimal result since the algorithm searchs from high E_b/N_0 and low code rate to low E_b/N_0 and high code rate.

Algorithm 1 Symbol-Wise EXIT Chart Based Two-Stage Optimization Algorithm for NB-LDPC Coded PDMA

Input: Target code rate R_T, sufficiently low initial code rate $0 < R_c < R_T < 1$, sufficient high E_b/N_0, maximum variable node degree D_v, maximum check node degree D_c, the prefix number of optimization iterations $N\_iter = 3$;

Output: degree distribution pair $(\boldsymbol{\lambda}, \boldsymbol{\rho})$, code rate R;

Initialize $\lambda_3 = 1.0$, $\rho_j = 1.0$, where $j = \lfloor 3/(1 - R_c) \rfloor$;

for $n = 1 : N_{iter}$

Step 1: With check-degree profile fixed, optimize the variable node degree profile as follows,

$$\begin{aligned} \min \quad & \frac{1}{\sum_{i=2}^{Dv} (\lambda_i / i)} \\ s.t. \quad & f_1\left(I_A^{(I)}\right) > f_2^{-1}\left(I_A^{(I)}\right) \text{ for } I_A^{(I)} \in [0, 1] \\ & \lambda_i \geq 0 \quad \text{for} \quad 2 \leq i \leq D_v \\ & \sum_{i=2}^{Dv} \lambda_i = 1 \end{aligned}$$

Step 2: With the variable node degree profile fixed, optimize the check node degree profile as follows,

$$\begin{aligned} \min \quad & \sum_{j=3}^{Dc} (\rho_j / j) \\ s.t. \quad & f_1\left(I_A^{(I)}\right) > f_2^{-1}\left(I_A^{(I)}\right) \text{ for } I_A^{(I)} \in [0, 1] \\ & \rho_j \geq 0 \quad \text{for} \quad 3 \leq j \leq D_c \\ & \sum_{j=3}^{D_c} \rho_j = 1 \end{aligned}$$

Step 3: calculate the code rate R, if $|R - R_T| \leq 0.05$, jump to step **Return**, otherwise $E_b/N_0 = E_b/N_0 - 0.1$ and jump to step 1.

end for

Return degree profile pair$(\boldsymbol{\lambda}, \boldsymbol{\rho})$, code rate R and threshold SNR E_b/N_0.

V. SIMULATION RESULTS AND DISCUSSION

A. OPTIMIZATION RESULTS AND BER COMPARSION

In this section, we obtain two irregular GF(4)-LDPC codes, denoted as code 1 and code 2 whose key parameters are shown in Table 1, with the proposed optimization algorithm for 150% and 200% overload cases respectively. In Table 1, code 3 denotes the irregular GF(4)-LDPC code with the same degree distribution as World Interoperability for Microwave Access (WiMax) LDPC code but with code length of $N_s = 9600$ and random constructed [21], [22]. Fig.7 shows the EXIT-chart of the PDMA systems with regular-(3,6) GF(4)-LDPC, irregular GF(4)-LDPC code (with the same degree distribution as WiMax LDPC, denoted as code 3 as shown in Table 1), and the optimized irregular LDPC code (code 1) respectively. In Fig. 7(a), with regular-(3,6) GF(4)-LDPC, the threshold SNR predicted by SEXIT in terms of E_b/N_0 is 4.9dB. In Fig. 7(b), the threshold $E_b/N_0 = 4.2$dB with code 3. While in Fig. 7(c) the optimized irregular LDPC (code 1) proposed in this work with threshold $E_b/N_0 = 3.3$dB as predicted by SEXIT.

TABLE 1. Three degree distribution pairs of GF(4)-LDPC.

Code 1		Code 2		Code 3 (WiMax degree distribution)	
i	λ_i	i	λ_i	i	λ_i
2	0.4670	2	0.5286	2	0.2895
3	0.2835	3	0.1368	3	0.3158
9	0.1710	16	0.0476	6	0.3947
10	0.0785	17	0.2870		
j	ρ_j	j	ρ_j	j	ρ_j
5	0.3287	6	0.9612	6	0.6316
6	0.6713	7	0.0388	7	0.3684
$R = 0.4994$		$R = 0.4970$		$R = 0.5$	
$E_b/N_0 = 3.3$dB		$E_b/N_0 = 5.3$dB		$E_b/N_0 = 4.2$dB in $\mathbf{S}_{2,3}$ case $E_b/N_0 = 6.6$dB in $\mathbf{S}_{3,6}$ case	

In order to verify the effectiveness of the proposed optimization algorithm, we constructed three GF(4)-LDPC codes according to the corresponding degree distributions as shown in Table 1 and a regular-(3,6) GF(4)-LDPC code. All codes are of length $N_s = 9600$ symbols over GF(4) and are of code rate $R = 0.5$. The nonzero elements of theirs pairty check matrix are chosen from the nonzero elements of GF(4) randomly. The WiMax LDPC (code 3) has maximum variable node degree $D_v = 6$ while the optimized irregular LDPC code, code 1 and code 2, with $D_v = 10$ and $D_v = 17$ respectively. In all simulation settings, QPSK modulation is employed and identical independent fading channel model is used. Meanwhile, we assume that channel fading coefficients are perfectly known at the receiver side but not known at the transmitters. In both Fig. 8 and Fig.9, the number of outer iterations $Out\_Iter = 15$, the number of iterations of GAMP/SMP detector $In\_iter = 6$, and the number of iterations of LDPC decoder is set to 30. The outer iteration denotes the message exchanging between detector and LDPC decoder, while the inner iteration denotes the message exchanging between the VNDs and FNDs within SMP/GAMP detector. In Fig. 8, the numerical simulation results for 150% overload PDMA system with PM $\mathbf{S}_{2,3}$ are shown. We found that the optimized irregular GF(4)-LDPC code (code1) outperforms regular-(3,6) GF(4)-LDPC code about 1.4dB at bit error ratio (BER) level of 1e-5. Furthermore, the optimized irregular GF(4)-LDPC has about 0.5dB performance gain than code 3. Fig. 9 shows the BER simulation results of 200% overload PDMA system with PM $\mathbf{S}_{3,6}$. The proposed irregular GF(4)-LDPC (code 2) coded system outperforms the regular-(3,6) GF(4)-LDPC coded one 3dB while outperforms code 3 coded system about 1dB at the BER level of 1e-5. When system overload becomes larger, the performance gain introduced by the proposed algorithm becomes more prominent.

We also give a comparison between the GF(4)-LDPC coded scheme and GF(2)-LDPC coded system as shown in Fig. 10. The threshold E_b/N_0 of WiMax LDPC (binary code in [22]) coded PDMA with PM $\mathbf{S}_{2,3}$ and QPSK is 3.9dB. When we constrain the $D_v = 10$ and $D_c = 10$ for comparison purpose, then the threshold E_b/N_0 (predicted by EXIT chart as reference [18]) of the optimized GF(2)-LDPC is also 3.9dB. In Fig. 10, the green solid line with square marker denotes the BER of optimized GF(2)-LDPC code with degree distribution and with code-length of $N_b = 2304$bits.

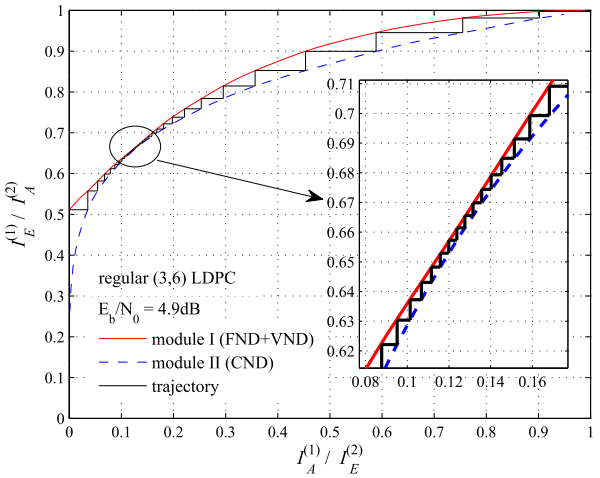

(a)

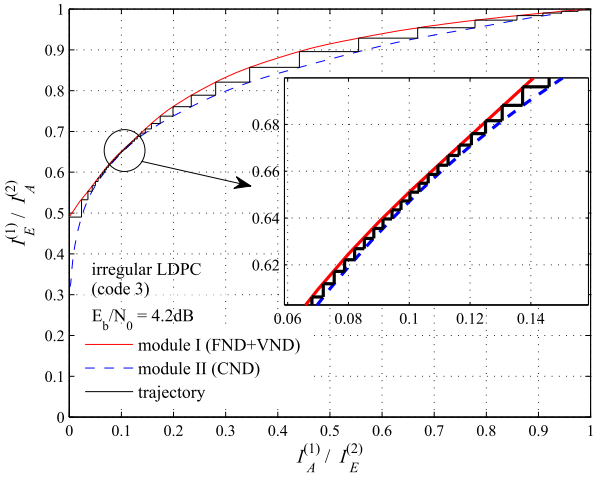

(b)

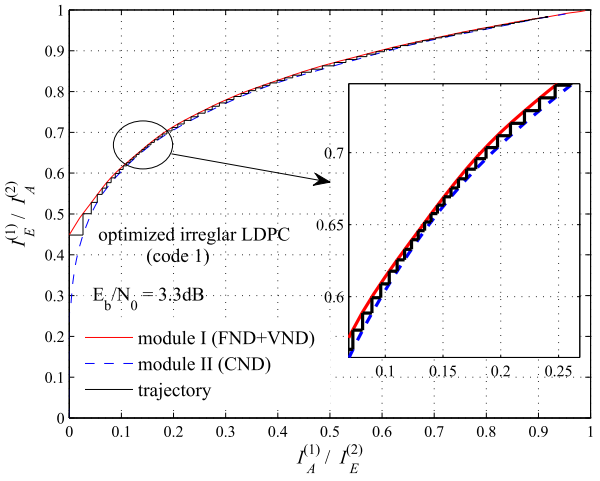

(c)

FIGURE 7. EXIT chart of three GF(4)-LDPC coded PDMA (a) regular-(3,6) GF(4)-LDPC coded PDMA (b) irregular GF(4)-LDPC (code 3) coded PDMA (c) optimized irregular GF(4)-LDPC (code 1) coded PDMA.

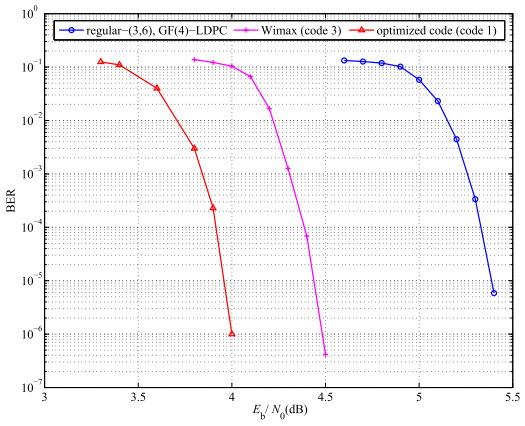

FIGURE 8. BER performance comparison of GF(4)-LDPC coded PDMA with $S_{2,3}$ PM.

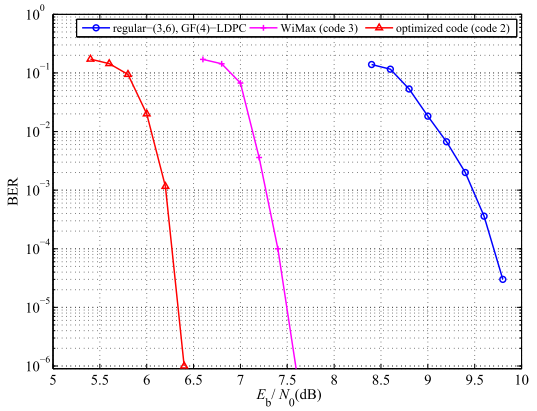

FIGURE 9. BER performance comparison of GF(4)-LDPC coded PDMA with $S_{3,6}$ PM.

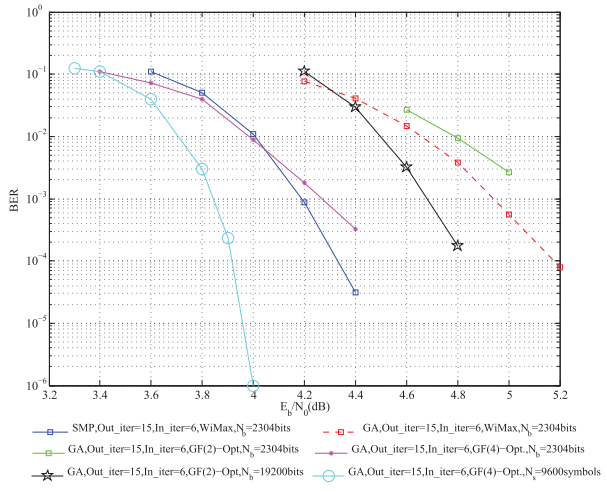

FIGURE 10. BER performance comparison between GF(4)-LDPC coded PDMA and GF(2)-LDPC code ones with $S_{2,3}$ PM and QPSK.

We find that the optimized GF(2)-LDPC code exhibits about the same BER performance as WiMax code with the same code-length. For the optimized GF(4)-LDPC code (code 1), when its code length $N_s = 1152$ symbols, with GAMP-based

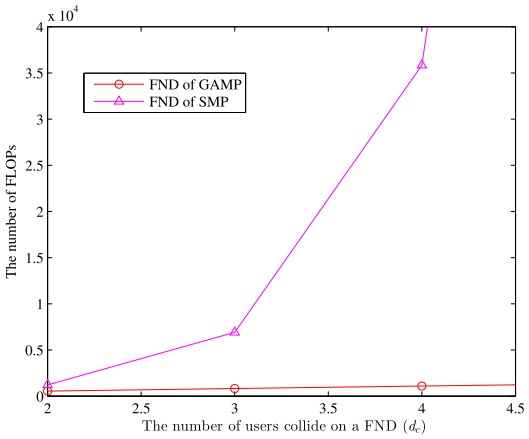

FIGURE 11. FND complexity comparison between GAMP-based and SMP-based detector.

detector (marked with GA as in Fig. 10), it outperforms both the WiMax LDPC code and optimized GF(2)-LDPC code system with GAMP about 1dB respectively, and achieves about the same performance as WiMax coded PDMA with SMP-based detector. Furthermore, when the code length of the GF(4)-LDPC code increases to $N_s = 9600$symbols, it performs about 0.9dB better than the optimized GF(2)-LDPC code with length $N_b = 19200$bits at the BER level of 1e-4.

B. COMPLEXITY COMPARISON

In this subsection, we give a simple comparison between the GF(4)-LDPC coded PDMA with GAMP detector and GF(2)-LDPC coded PDMA with SMP detector. The bottle-neck of the SMP algorithm is the computation complexity of underling chip wise MAP of FND, which need to compute $|\mathcal{A}|^{d_c}$ Euclidean distance be of the form $|y_j - h_{j,i}x_i - \sum_{i'\neq i} h_{j,i'}x_{i'}|^2$ with all x_i fixed, $1 \leq i \leq d_c$. Thus the computational complexity is $8(d_c+3)|\mathcal{A}|^{d_c}$ floating point of operations (FLOPs) for each FND. While the computational complexity of GAMP algorithm of the FND, according to [5], is $17|\mathcal{A}|d_c$. Fig. 11 shows the relationship between the number of FLOPs and the number of users (d_c) collide on a specific RE. When $d_c = 4$, such as PM $\mathbf{S}_{3,6}$ case, the complexity of GAMP is about only 1/32 of that of SMP algorithm. For LDPC code, when forward and backward based log-domain belief propagation decoding algorithm is employed, the computational complexity of CND is proportional to q^2 and $3d_c - 2$. So the computation complexity of GF(4)-LDPC is about 4 times of GF(2)-LDPC code conditioned on the same D_c. Meanwhile, the GF(4)-LDPC decoder needs about 50% more memories than GF(2)-LDPC. For the code 1, code 2 and code 3 in Table 1, they are of the similar decoding complexity since they have about the same maximum check node degree.

VI. CONCLUSION

In this work, we have proposed a non-binary LDPC coded PDMA scheme. By combining the symbol-wise mapping

from the non-binary code symbol to modulation constellation and an symbol-wise multiuser detection algorithm, a seamless information transfer IDD receiver is achieved at the receiver side. Compared with the existing work, the proposed scheme in this paper is of good performance and has relatively low front-end detection complexity while keep the computational complexity of the channel decoder at an reasonable level. The proposed GF(4)-LDPC coded PDMA scheme is of practical importance for future wireless applications.

REFERENCES

[1] J. van de Beek and B. M. Popovic, "Multiple access with low-density signatures," in *Proc. IEEE Global Telecommun. Conf. (GLOBECOM)*, Nov. 2009, pp. 1–6.
[2] R. Razavi, M. Al-Imari, M. A. Imran, R. Hoshyar, and D. Chen, "On receiver design for uplink low density signature OFDM (LDS-OFDM)," *IEEE Trans. Commun.*, vol. 60, no. 11, pp. 3499–3508, Nov. 2012.
[3] X. Dai, S. Chen, S. Sun, S. Kang, Y. Wang, Z. Shen, and J. Xu, "Successive interference cancelation amenable multiple access (SAMA) for future wireless communications," in *Proc. IEEE Int. Conf. Commun. Syst.*, Nov. 2014, pp. 222–226.
[4] T. L. Narasimhan and A. Chockalingam, "Detection and decoding in large-scale MIMO systems: A non-binary belief propagation approach," in *Proc. IEEE 79th Veh. Technol. Conf. (VTC Spring)*, May 2014, pp. 1–5.
[5] S. Wu, L. Kuang, Z. Ni, J. Lu, D. Huang, and Q. Guo, "Low-complexity iterative detection for large-scale multiuser MIMO-OFDM systems using approximate message passing," *IEEE J. Sel. Topics Signal Process.*, vol. 8, no. 5, pp. 902–915, Oct. 2014.
[6] M. C. Davey and D. MacKay, "Low-density parity check codes over GF(q)," *IEEE Commun. Lett.*, vol. 2, no. 6, pp. 165–167, Jun. 1998.
[7] A. Voicila, D. Declercq, F. Verdier, M. Fossorier, and P. Urard, "Low-complexity decoding for non-binary LDPC codes in high order fields," *IEEE Trans. Commun.*, vol. 58, no. 5, pp. 1365–1375, May 2010.
[8] L. Conde-Canencia, A. Al-Ghouwayel, and E. Boutillon, "Complexity comparison of non-binary LDPC decoders," ICT-MobileSummit, Santander, Boadilla del Monte, Spain, Tech. Rep., 2009.
[9] R. Hoshyar, F. P. Wathan, and R. Tafazolli, "Novel low-density signature for synchronous CDMA systems over AWGN channel," *IEEE Trans. Signal Process.*, vol. 56, no. 4, pp. 1616–1626, Apr. 2008.
[10] *Technical Specification Group Radio Access Network; Evolved Universal Terrestrial Radio Access (EUTRA); Multiplexing and Channel Coding*, document TS 36.212, Version 9.1.0, 3GPP, 2010.
[11] X. Dai, Z. Zhang, B. Bai, S. Chen, and S. Sun, "Pattern division multiple access: A new multiple access technology for 5G," *IEEE Wireless Commun.*, vol. 25, no. 2, pp. 54–60, Apr. 2018.
[12] F. R. Kschischang, B. J. Frey, and H.-A. Loeliger, "Factor graphs and the sum-product algorithm," *IEEE Trans. Inf. Theory*, vol. 47, no. 2, pp. 498–519, 2001.
[13] P. Bromiley, "Products and convolutions of Gaussian probability density functions," *Tina-Vision Memo*, vol. 3, no. 4, p. 1, 2003.
[14] T. P. Minka, "A family of algorithms for approximate Bayesian inference," Ph.D. dissertation, Massachusetts Inst. Technol., Cambridge, MA, USA, 2001.
[15] S. ten Brink, G. Kramer, and A. Ashikhmin, "Design of low-density parity-check codes for modulation and detection," *IEEE Trans. Commun.*, vol. 52, no. 4, pp. 670–678, Apr. 2004.
[16] A. Bennatan and D. Burshtein, "Design and analysis of nonbinary LDPC codes for arbitrary discrete-memoryless channels," *IEEE Trans. Inf. Theory*, vol. 52, no. 2, pp. 549–583, Feb. 2006.
[17] J. Kliewer, S. X. Ng, and L. Hanzo, "On the computation of exit characteristics for symbol-based iterative decoding," in *Proc. 4th Int. Symp. Turbo Codes Rel. Topics, 6th Int. ITG-Conf. Source Channel Coding*. Frankfurt, Germany: VDE, 2006, pp. 1–6.
[18] J. Xu, X. Han, H. Ding, Z. Li, Z. Yu, and X. Dai, "Optimisation of convergence-aware coded PDMA for 5G wireless systems," *IET Commun.*, vol. 13, no. 2, pp. 243–250, Jan. 2019.
[19] T. Richardson and R. Urbanke, *Modern Coding Theory*. Cambridge, U.K.: Cambridge Univ. Press, 2008.
[20] S. Boyd, S. P. Boyd, and L. Vandenberghe, *Convex Optimization*. Cambridge, U.K.: Cambridge Univ. Press, 2004.
[21] B. Cristea, "Turbo receivers with IT++," in *Proc. 2nd Int. Conf. Simulation Tools Techn.*, 2009, pp. 1–7.
[22] *IEEE Standard for Local and Metropolitan Area Networks—Part 16: Air Interface for Fixed and Mobile Broadband Wireless Access Systems*, IEEE Standard 802.16-2004, Dec. 2005.

HANQING DING received the B.E. degree in information and communication engineering and the Ph.D. degree in military communication from Xidian University, Xian, China, in 2001 and 2011, respectively. He is currently an Associate Professor with the School of Computer and Communication Engineering, Zhengzhou University of Light Industry, Zhengzhou, China. His research interests include wireless communications, resource allocation, and deep learning.

QINGQING LIU is currently pursuing the Ph.D. degree in information and communication engineering with the Beijing Institute of Technology, Beijing. Her research interests include stochastic signal processing and digital communication.

ZIHANG DING is currently a Student with the International Education College, Zhengzhou University of Light Industry, Zhengzhou, China. Her research interests include information systems and software engineering.

JIN XU received the B.E. degree in electronic and information engineering from Zhengzhou University, in 2005, the M.S. degree in communication and information system from the Wuhan University of Technology, in 2011, and the Ph.D. degree from the Beijing University of Posts and Telecommunications, Beijing, China, in 2015. He is currently a Lecturer with the School of Computer and Communication Engineering, Zhengzhou University of Light Industry, Zhengzhou. His research interests include LDPC code, iterative decoding algorithm, MIMO detection, and non-orthogonal multiple access.

ZHE ZHANG received the B.E. degree in electronic and information engineering from The First Aviation Academy of Chinese Air Force, Xinyang, China, in 2009, and the Ph.D. degree in information and communication engineering from Zhengzhou University, Zhengzhou, in 2017. She is currently a Lecturer with the School of Computer and Communication Engineering, Zhengzhou University of Light Industry, Zhengzhou. Her research interests include radio resource management and signal processing for wireless communications.

WEIHUA LIU (Member, IEEE) received the M.S. degree in applied mathematics from Zhengzhou University, Zhengzhou, China, in 2014, and the Ph.D. degree in communication and information system from the University of Chinese Academy of Sciences, Beijing, China, in 2018. He is currently a Lecturer with the School of Computer and Communication Engineering, Zhengzhou University of Light Industry, Zhengzhou. His research interests include information theory, wireless communication, and interference management.

XUEYAN CHEN received the B.S. degree in electronic and information engineering from PLA Information Engineering University, in 2009, and the M.S. degree from Shenyang Ligong University and the Ph.D. degree from the Beijing University of Posts and Telecommunications (BUPT), in 2012 and 2018, respectively. She is currently a Lecturer with the School of Computer and Communication Engineering, Zhengzhou University of Light Industry, Zhengzhou, China. Her research interests include cognitive radio, relay systems, physical layer security, and energy harvesting.